Journal of New Materials for Electrochemical Systems 17, 257-263 (2014)

Optimization of Parameters and Microstructural Properties of $Ba_{0.5}Sr_{0.5}Co_{0.8}Fe_{0.2}O_{3-\delta}$ Thin Films Grown by Pulsed Laser Deposition (PLD)

Saša Zeljković[1], Toni Ivas[2], Anna Infortuna[2] and Ludwig J. Gauckler[1]

[1]University of Banja Luka, Faculty of Natural Sciences and Mathematics, Banja Luka, Bosnia and Herzegovina
[2]ETH Zürich, Department of Materials, Zürich, Switzerland

Received: April 08, 2014, Accepted: August 10, 2014, Available online: November 20, 2014

Abstract: *$Ba_{0.5}Sr_{0.5}Co_{0.8}Fe_{0.2}O_{3-\delta}$ thin films were grown by pulsed laser deposition (PLD) in the temperature range from room temperature (RT) to 1073 K and at oxygen pressures from 6.66 to 39.99 Pa in order to produce dense defect-free thin films. Si with a native oxide layer and MgO were used as the substrate materials. The structure of the thin films was highly dependent on substrate temperature, material and oxygen partial pressure, leading to formation of different microstructures – pores, cracks, columnar and fibrous grains. Cracks and delamination of the thin films were observed in dense layers at higher temperatures, while this was not the case with the columnar thin films. Differences in thermal expansion coefficient, phase transformation and oxygen non-stoichiometry of BSCF are possible explanations for the cracking of the dense thin films. Thin films with a columnar structure are positively influenced by annealing inducing grain growth and densification.*

Keywords: $Ba_{0.5}Sr_{0.5}Co_{0.8}Fe_{0.2}O_{3-\delta}$ (BSCF), Pulsed laser deposition (PLD), Surface structure, Thin films.

1. INTRODUCTION

$Ba_{0.5}Sr_{0.5}Co_{0.8}Fe_{0.2}O_{3-\delta}$ (BSCF) composite oxide has attracted considerable attention as an oxygen separation membrane [1] and as a low temperature solid oxide fuel cell (SOFC) cathode material [2]. This ceramic material is a mixed electronic and ionic conductor with a perovskite structure [3].

Thin film deposition as applied to micro-solid oxide fuel cell (μSOFC) fabrication is an emerging and highly active field of research that is attracting greater attention [4]. Thin films of mixed-conducting materials are considered important due to their potential application in μSOFCs [5]. Miniaturization of SOFCs is desirable because portable devices have an increasing demand for energy, and in comparison μSOFCs have, by several orders, a higher energy density than conventional batteries [6].

Pulsed laser deposition (PLD) is a physical method of thin film deposition in which a high power pulsed laser beam is focused inside a vacuum chamber to ablate a target composed of the desired thin film material, which is then to be deposited onto a substrate. Pulsed laser deposition is used to produce thin films of many materials because of the preservation of the stoichiometry from target to the thin film [7]. The control over the desirable structure of the grown thin films can be achieved by variation of pressure and substrate temperature, pulse energy, wavelength and substrate – target distance which could lead to dense films without significant defects, pores and cracks.

Baumann *et al*. [8] reported the fabrication of dense BSCF films on top of polished 9.5 mol% Y_2O_3-doped ZrO_2 (YSZ) single crystals at a repetition frequency of 5 Hz, deposition rate of 8 nm/min, in a 40 Pa oxygen atmosphere, while the substrate was kept at a temperature of 1043 K. The authors also reported that, following deposition, the films with a thickness of 100 (±10) nm were annealed at 923 K for 30 min in 10^5 Pa oxygen.

Recently, Burriel et al. [9] deposited epitaxial BSCF thin films on $NdGaO_3$ single crystal substrate followed by evaluation of the electrical conductivity properties as well as surface exchange coefficients.

We have investigated the microstructure of BSCF thin films deposited on Si with a native oxide layer and MgO substrates by pulsed laser deposition (PLD) in the temperature range from RT to 1073 K and at oxygen pressures from 6.66 to 39.99 Pa in order to understand its influence on the thin film properties and in order to produce dense defect-free thin films (Table 1). An additional goal

*To whom correspondence should be addressed: Email: sasa.zeljkovic@unibl.rs
Phone: + 387 65 596 980

was the investigation of the annealing influence on the thin film microstructure, densification and crystal structure.

2. EXPERIMENTAL

The BSCF target for PLD was made from $Ba_{0.5}Sr_{0.5}Co_{0.8}Fe_{0.8}O_{3-\delta}$, 99.9%, Praxair powder. The powder (10.00g) was first pressed in the uniaxial press for two minutes under a pressure of 14.6 MPa, and afterwards in the isostatic press for 2.5 minutes under a pressure of 582.4 MPa, turning it into a round pellet. The pellet was sintered at 1373 K for 6 hours. Heating/cooling rates were $3Kmin^{-1}$. XRD measurements confirmed a single-phase $Ba_{0.5}Sr_{0.5}Co_{0.8}F$ - $e_{0.2}O_{3-\delta}$ perovskite structure.

The films were deposited in the PLD facility with a PLD workstation (Surface, Hueckelhoven, Germany). The BSCF target was irradiated at a 10 Hz repetition rate from a KrF excimer laser with a wavelength of 248 nm. The pulse energy was 200 and 250 mJ with pulse duration of 25 ns. During the experiments it was observed that the change in energy of the laser beam does not significantly change the plume characteristics.

The target-substrate distance was adjusted from 55 to 70 mm with beam cross-section 8x17 mm^2. It has been concluded that a distance of 55 mm together with laser energy of 250 mJ gives the optimal results as well as an absence of clusters. Target rotation was held at 10 rpm. In some experiments the substrate was also rotated up to 10 rpm, which gave better thickness uniformity.

The substrate was heated up to 1073 K by an oxygen compatible furnace; the temperature distribution was uniform on a circular area with a diameter of 2“. The heating rate in all experiments (in which a heating step occurred) was held to 10 K/min.

Background pressure of oxygen was 6.66 – 39.99 Pa, obtained by a turbo molecular pump. Also, the pulse number directly influenced the thickness of the thin film. It was considered that each pulse deposits 0.1 nm of the material. Thin films were deposited on the silicon with native oxide and on the MgO.

Thin films and pellets have been characterized with a LEO Gemini 1530 FEG-SEM. For most of the experiments the acceleration voltage was set to 3 kV.

For measuring diffractograms of pellets, thin films and powders, a SIEMENS D-5000 diffractometer with Cu-Kα X-ray tube (λ=154 nm) and Θ-2Θ configuration was used. All measurements had a range from 5˚ (15˚ for experiments at the beginning of work) to 75˚ and a step of 0.05˚.

For thermal analysis a NETZSCH STA 449 C Jupiter equipped with Rhodium-Platinum furnace was used. The gas flows were controlled by Bronkhorst flow meters with magnetic valves.

3. EXPERIMENTAL RESULTS AND DISCUSSION

3.1. Influence of substrate temperature and oxygen partial pressure

The microstructure of the thin film was influenced by various factors during deposition process. At most, thin film surface structure was influenced by pressure, temperature of substrate, frequency of the laser beam, and substrate material.

From the structural zone model proposed by Thornton [10] it is known that there are four zones in the pressure-temperature diagram. In the Thornton diagram, the T zone (transition zone) is the most favorable. The T zone consists of dense fibrous grains. According to Thornton, Zone 1 consists of tapered crystals with domed tops, which are separated by voided boundaries. The internal structure of the crystals has a high density of defects. Zone 2 consists of columnar grains separated by distinct, dense, intercrystalline boundaries; the surface has a smooth matte appearance. Zone 3 consists of equiaxed grains with a bright surface. The structure and properties correspond to a fully annealed metal.

The Thornton diagram, which has been used as an orientation for experiments, showed that the T zone represents the thin films as required.

In line with the Thornton results is the fact that thin films deposited at RT and in 39.99 Pa of oxygen (Figure 1(a)–(b)) had a columnar structure with big grains of poorly diffused material. During deposition, the substrate was not heated enough to ensure the surface mobility. The structure was porous and the density of this film was low. The thin film deposited at 673 K in 6.66 Pa of oxygen (Figure 1(c)) had a denser structure compared to the thin film deposited at room temperature. The same thin film has been annealed at 973 K. The SEM image made after the annealing experiment

Table 1. $Ba_{0.5}Sr_{0.5}Co_{0.8}Fe_{0.2}O_{3-\delta}$ deposition conditions

Experiment number	01	02	03	04	05	06	07	08
Energy [mJ]	210	250	250	250	250	210	250	200
Frequency [Hz]	10	10	10	10	10	10	10	10
Temperature [K]	673	873	873	673	673	RT	673	1073
Heating rate [$Kmin^{-1}$]	10	10	10	10	10	-	10	10
Pulse number [k]	20	50	50	50	50	10	50	50
Oxygen pressure [Pa]	6.66	6.66	13.33	13.33	13.33	39.99	6.66	6.66
Target rotation [rpm]	10	10	10	10	10	10	10	10
Substrate rotation [rpm]	-	-	-	-	-	-	-	-
Substrate distance [cm]	6.5	6.5	6.5	6.5	6.5	5.5	6.5	6.5
Substrate material	Si	Si	Si	Si	Si	Si	MgO	MgO

Experiment number	09	10	11	12	13	14	15	16
Energy [mJ]	200	250	200	250	250	250	250	250
Frequency [Hz]	10	10	10	10	10	10	10	10
Temperature [K]	1073	673	673	573	873	1073	973	873
Heating rate [$Kmin^{-1}$]	10	10	10	10	10	10	10	10
Pulse number [k]	50	100	100	100	100	100	150	100
Oxygen pressure [Pa]	6.66	6.66	6.66	26.66	26.66	26.66	26.66	26.66
Target rotation [rpm]	10	10	10	10	10	10	10	10
Substrate rotation [rpm]	-	10	-	10	10	10	10	10
Substrate distance [cm]	6	6.5	5.5	5.5	5.5	5.5	5.5	7
Substrate material	MgO/Si	MgO/Si	MgO	Si	Si	Si	Si	Si

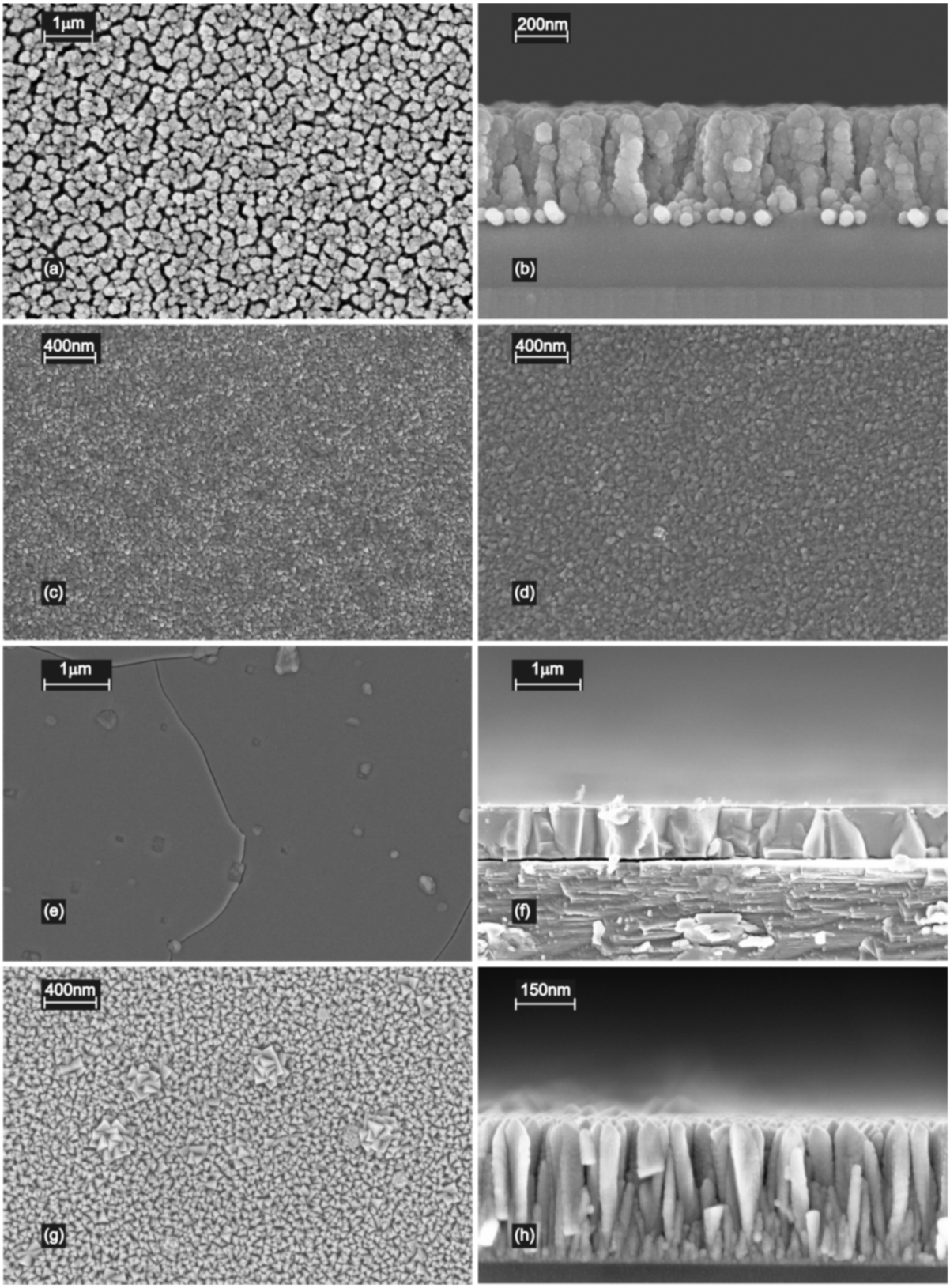

Figure 1. SEM morphologies of the $Ba_{0.5}Sr_{0.5}Co_{0.8}Fe_{0.2}O_{3-\delta}$ thin films deposited on (a) Si at RT in 39.99 Pa of O_2, sectional view, (b) Si at RT in 39.99 Pa of O_2, cross-section, (c) MgO at 673 K in 6.66 Pa of O_2, sectional view, (d) MgO at 673 K in 6.66 Pa of O_2 after annealing (973K), sectional view, (e) MgO at 1073 K in 6.66 Pa of O_2, sectional view, (f) MgO at 1073 K in 6.66 Pa of O_2, cross-section, (g) Si at 873 K in 26.66 Pa of O_2, sectional view, (h) Si at 873 K in 26.66 Pa of O_2, cross-section.

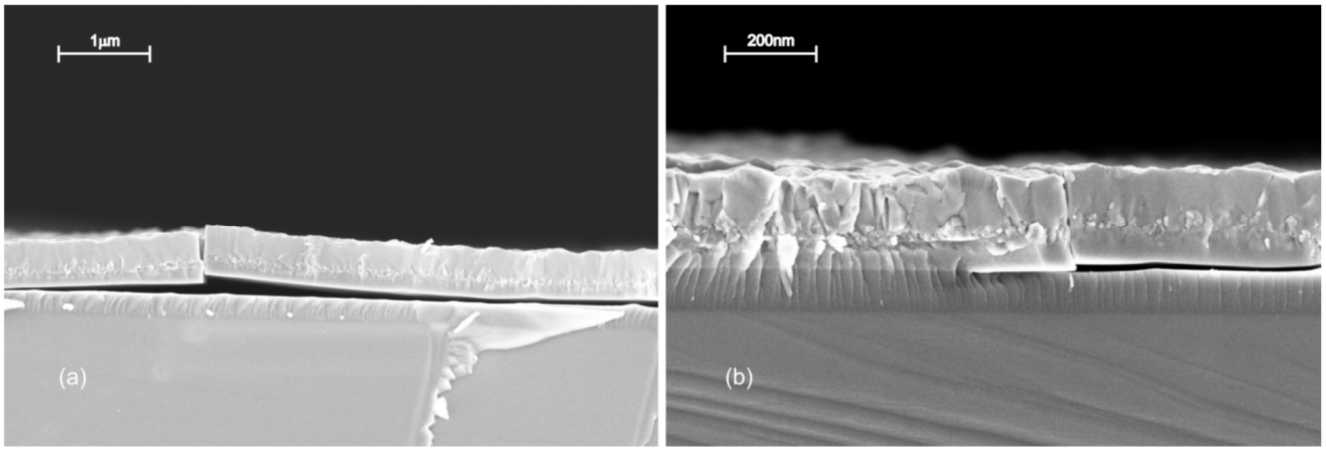

Figure 2. Sectional SEM morphologie of the $Ba_{0.5}Sr_{0.5}Co_{0.8}Fe_{0.2}O_{3-\delta}$ thin film deposited on Si at 1073 K in 26.66 Pa of O_2 (experiment 14).

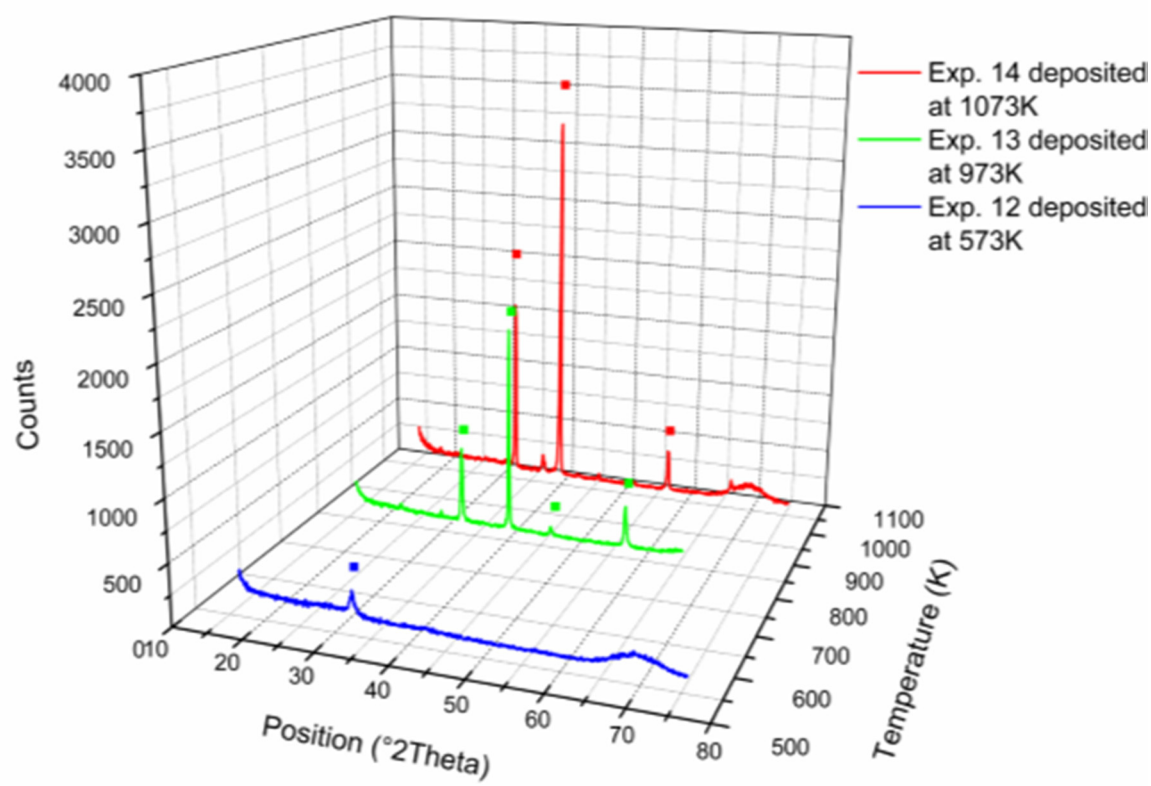

Figure 3. Diffractograms of $Ba_{0.5}Sr_{0.5}Co_{0.8}Fe_{0.2}O_{3-\delta}$ deposited at 573 K (experiment 12), 873 K (experiment 13) and 1073 K (experiment 14) with marked $Ba_{0.5}Sr_{0.5}Co_{0.8}Fe_{0.2}O_{3-\delta}$ peaks.

showed densification of the film and bigger grains compared to the material before the annealing (Figure 1(d)). Thin films deposited at 873 K in 26.66 Pa of oxygen had a columnar structure (Figure 1(g)-(h)) with closely packed columnar grains. With increasing temperature the structure of the thin film changed from larger grain and fibrous – columnar structure to a fully dense surface. Full densification and transition from columnar to fully dense structure takes place between 973 and 1073 K. Thin films deposited at 1073 K in 6.66 Pa of oxygen onto a MgO substrate were dense but also cracked and delaminated (Figure 1(e)-(f)). The exact temperature at which cracking occurred is not known. Thin films deposited at 1073 K in 26.66 Pa of oxygen onto a Si substrate (Figure 2(a)-(b)) were dense and more delaminated than the thin films deposited onto a MgO. On the sites where the thin film was not separated from the substrate zone slight diffusion, 400 nm thick could be seen (in BSCF and Si layer).

The crystal structure of the thin films changed with the deposition temperature. The number of peaks assigned to

$Ba_{0.5}Sr_{0.5}Co_{0.8}Fe_{0.2}O_{3-\delta}$ X-ray spectra was increasing with the substrate temperature during thin film deposition (Figure 3).

3.2. Cracking of the dense thin films

The expansion of the lattice in the perovskite structures are mainly attributed to a phase transformation [11,12,13,14], thermal expansion due to increasing temperature (DT) and chemical expansion [15]. It was found that the phase transformation starts at 1073 K with hexagonal phase formed - primarily in grain boundaries, and after the saturation of boundary nucleation sites, phase transition also occurred within the matrix. [16,17,18] The chemical expansion is caused by a decrease in oxygen stoichiometry (Dd) associated with an increase of ionic radius upon reduction of the B site cations with increasing temperature and decreasing oxygen partial pressure. The chemical, thermal, and total linear strains are defined as:

$$\varepsilon_c = \left.\frac{(a-a_0)}{a_0}\right|_{T=const}$$
$$\varepsilon_{Th} = \left.\frac{(a-a_0)}{a_0}\right|_{\delta=const} \quad (1)$$
$$\varepsilon_T = \left.\frac{(a-a_0)}{a_0}\right|_{p_{O_2}=const}$$

where a is the lattice parameter and a_o is the lattice parameter in the reference state. Analogously to Equation the chemical, thermal, and total expansions are defined as $\varepsilon_c / \Delta\delta$, $\varepsilon_{Th} / \Delta T$, and $\varepsilon_T / \Delta T$.

McIntosh *et al*. [19] measured the chemical and thermal expansion of BSCF between 873 and 1173 K in oxygen partial pressures between 1×10^{-3} and 1 atm. The measured thermal and chemical expansion coefficients are 19.0(5)-20.8(6) $\times10^{-6}$ $K^{-1}$and 0.016(2)-0.026(4) $\times10^{-6}$ K^{-1}, respectively.

By considering the distribution of the stresses in the thin film as a simple model of a bimetallic strip where two layers of materials with different thermal expansion coefficients are tightly bonded, stress is defined as [20]:

$$\sigma_{xx1} = \frac{2E_1w^2\Delta T}{D}\left[2\left(E_1\alpha_1h_1+E_2\alpha_2h_2\right)\left(E_1h_1^3+E_2h_2^3\right)\right]-\frac{3}{2}\left(E_2\alpha_2h_2^2-E_1\alpha_1h_1^2\right)\left(E_2h_2^2-E_1h_1^2\right)$$
$$+y\frac{6E_1w^2\Delta T}{D}\left[\left(E_2\alpha_2h_2^2-E_1\alpha_1h_1^2\right)\left(E_1h_1+E_2h_2\right)-\left(E_1\alpha_1h_1+E_2\alpha_2h_2\right)\left(E_2h_2^2-E_1h_1^2\right)\right]-E_1\alpha_1\Delta T \quad (2)$$

Where E_i (i = 1,2) is the Young's modulus of the layer, w width of the layer, ΔT is the temperature change, h_i (i=1,2) is height of the layer, and α_i (i=1,2) is thermal expansion coefficient of the particular layer. The strain in this case is given by:

$$\varepsilon_o = \frac{2w^2\Delta T}{D}\left[2\left(E_1\alpha_1h_1+E_2\alpha_2h_2\right)\left(E_1h_1^3+E_2h_2^3\right)-\frac{3}{2}\left(E_2\alpha_2h_2^2-E_1\alpha_1h_1^2\right)\left(E_2\alpha_2^2-E_1\alpha_1^2\right)\right] \quad (3)$$

where ε_0 is a maximum strain at the bonding surface between the substrate and deposited film. The thermomechanical properties and dimensions of our PLD-sample are w = 8-10 mm, h_1 = 500 nm, h_2 = 500 mm, E_1=63.3 GPa (BSCF), E_2=248.17 GPa (MgO), $a_1=11.5\times10^{-6}$ K^{-1} (BSCF), and $a_2 = 9.83\times10^{-6}$ K^{-1} (MgO) [21]. Using the previous parameters and Equation the calculated maximum strain is ε_0 = 0.78% for the temperature change in our PLD process DT= 800 K. Thermal strain calculated from Equation is almost four times larger than the chemical strain of the BSCF measured by McIntosh *et al.* [19].

Cracking of the dense thin films deposited at 1073 K can thus be (apart from phase transition) attributed to differences in thermal expansion coefficient of the BSCF thin film and the substrate. Thermal expansion curves of dense BSCF samples show anomalous behavior with a sudden increase in the total expansion rate between 773 K and 923 K, due mainly to the loss of lattice oxygen caused by the reduction of Co^{4+} and Fe^{4+} to lower valence states [22-23]. Thermal expansion coefficients (TECs) of BSCF obtained by different groups are summarized in Table 2.

In order to examine the phase stability of the BSCF, DTA measurements were performed. The DTA experiment with $Ba_{0.5}Sr_{0.5}Co_{0.8}Fe_{0.2}O_{3-\delta}$ powder showed no signs of phase transformation, but this does not exclude the possibility of certain crystal structure transformations. During this experiment, powder was heated up to 1273 K with a heating rate of 10 K min^{-1}.

Cracks and delamination of the thin film were only noticed at higher temperatures and with dense layers. There were no cracks in the columnar thin films. Due to the grain boundary relaxation, thin films with fibrous and columnar grains did not show any cracks and delamination.

3.3. Effects of annealing on deposited thin films

Thin films deposited at 573 K and 873 K (experiments 12 and 13) were annealed at 873/973/1073 K to examine structural chang-

Table 2. Summary of the experimental results for TEC of the BSCF, together with calculated microstrain (see text, Equation (3)). Elastic module of the BSCF is E_1=63.3 GPa [22-23] and of MgO is E_2=248.17 GPa.

Chemistry	Temperature ranges			Microstrain (%)	Ref.
$Ba_{0.5}Sr_{0.5}$ $Co_{0.8}Fe_{0.2}O_3$	303-573 K	773-973 K	1073-303 K cooling		
x=0.00	16.2	22.1	19.7		[25]
x=0.10	14.4	26.7	19.6		
x=0.15	13.4	26.6	19.2	0.787	
x=0.20	13.1	25.4	18.7		
$Ba_{0.5}Sr_{0.5}Fe_{1-x}Co_xO_{3-\delta}$	873-1273 K	298-1273 K	1273-393 K cooling		
x=0.20	25.1	29.8	17.3		[24]
x=0.40	23.9	26.0	17.7		
x=0.60	26.4	24.5	18.2	0.787	
x=0.80	24.9	22.0	18.4		
$Ba_{0.5}Sr_{0.5}Co_{0.8}Fe_{0.2}O_{3-\delta}$	323-473 K	473-773 K	773-1173 K		
	16.92	13.85	16.74	0.786	[22-23]

All TEC data are given in $10^{-6}K^{-1}$

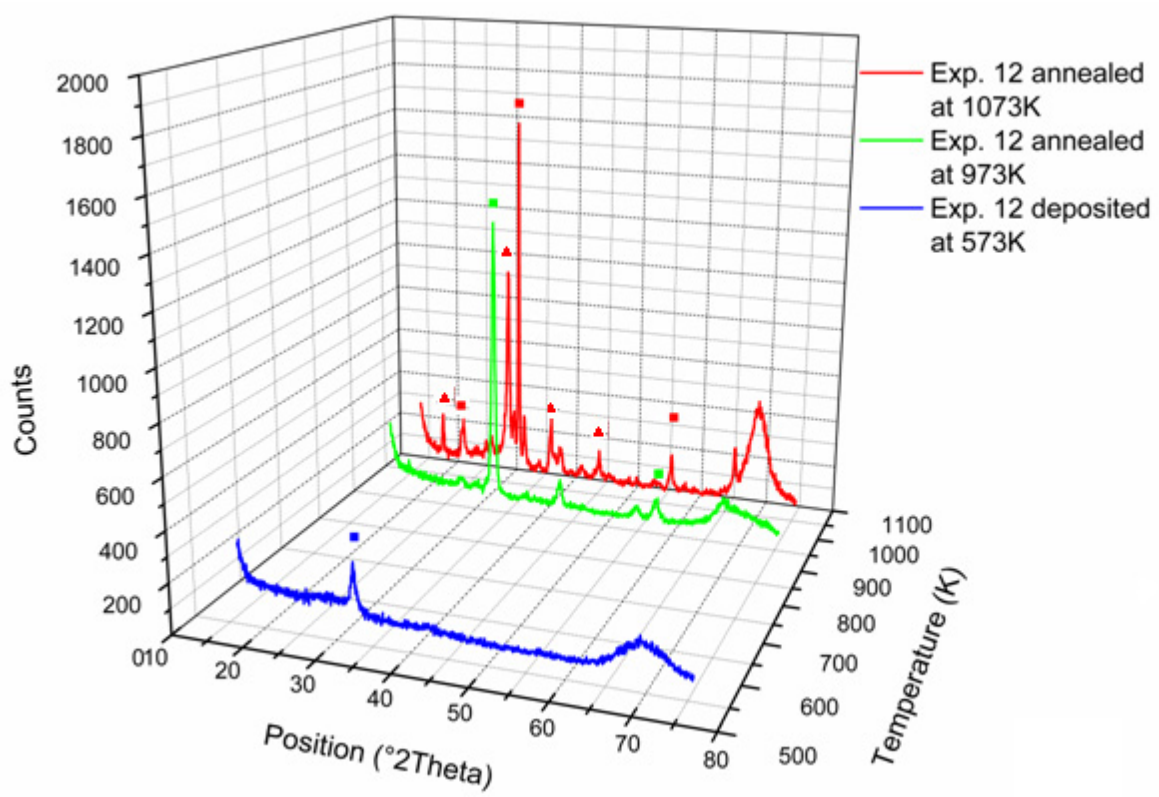

Figure 4. Diffractograms of $Ba_{0.5}Sr_{0.5}Co_{0.8}Fe_{0.2}O_{3-\delta}$ deposited at 573 K (experiment 12) and annealed at 973 K and 1073 K with marked $Ba_{0.5}Sr_{0.5}Co_{0.8}Fe_{0.2}O_{3-\delta}$ peaks of cubic (■) and hexagonal (▲) polymorphs.

es and possible differences compared to the thin films deposited at these temperatures.

XRD analysis was performed after deposition of the thin film, and after each step of annealing.

Annealing of the $Ba_{0.5}Sr_{0.5}Co_{0.8}Fe_{0.2}O_{3-\delta}$ produced significant changes in x-ray diffraction pattern of the resulting material, as can be seen in Figure 4. The cubic perovskite phase of BSCF transforms gradually, with increasing temperature, to a hexagonal polymorph.

4. CONCLUSIONS

In this work, we have explored the parameters for the deposition of thin and dense BSCF films produced by the PLD technique. The microstructure and morphology of the thin films varied, depending on the deposition factors – mainly substrate temperature and oxygen partial pressure.

Temperature has a major effect on the density and structure of the thin films while oxygen partial pressure in the range from 6.66 to 39.99 Pa affects the thin film expansion towards the substrate.

Dense, thin BSCF films, with thickness of 400 – 450 nm were produced at 1073 K in 6.66 Pa and 26.66 Pa of oxygen and were mainly separated from the substrate with visible deformations on the whole surface. The deformations clearly show that the thin film expanded more than the substrate. The thin film was delaminated to a large extent from the substrate surface with both substrates used (Si with a native oxide and MgO). More deformations were present under 26.66 Pa (Si substrate) than with the thin film deposited at the same temperature under 6.66 Pa of oxygen (MgO substrate). This could lead to the conclusion that low oxygen partial pressure together with high deposition temperature (1073 K) and a substrate with appropriate TEC could be responsible for the deposition of thin films with high density and without cracks.

Cracking and delamination of the dense BSCF thin films deposited at higher temperatures are most likely due to the phase transformation and previously disscussed difference in thermal expansion coefficient for BSCF and substrate material and oxygen non-stoichiometry of BSCF thin films. Nonexistence of cracks and delamination of thin films with a columnar structure is probably caused by the fact that columnar and fibrous grains relax due to the larger number of grain boundaries.

Thin films deposited at 573 K and 873 K and annealed at 873/973/1073 K were positively influenced by the annealing. The annealing process induced grain growth, densification and increased crystallization determined by XRD experiments before and after the annealing process.

For future research, the range of processing parameters must be extended in order to improve the microstructure of thin BSCF films and prevent cracking and delamination.

5. ACKNOWLEDGEMENTS

This research was done with the support of the Swiss Federal Commission for Scholarships for Foreign Students and the Ministry of Science and Technology of Republic of Srpska.

REFERENCES

[1] H. Wang, C. Tablet, A. Feldhoff and J. Caro, J. Memb. Sci., 262, 20 (2005).
[2] C.K. Dyer, J. Power Sources, 106, 31 (2002).
[3] Z. Shao and S. Haile, Nature, 431, 170 (2004).
[4] D. Beckel, A. Bieberle-Hütter, A. Harvey, A. Infortuna, U.P. Muecke, M. Prestat, J.L.M. Rupp and L.J. Gauckler, J. Power Sources, 173, 325 (2007).
[5] J. Fleig, H.L. Tuller and J. Maier, Solid State Ionics, 174, 261 (2004).
[6] A. Evans, A. Bieberle-Hütter, J.L. M. Rupp and L.J. Gauckler, J. Power Sources, 194, 119 (2009).
[7] R. Eason (Ed.), Pulsed Laser Deposition of Thin Films, John Wiley, Hoboken, New York, 2007.
[8] F.S. Baumann, J. Fleig, H.U. Habermeier and J. Maier, Solid State Ionics, 177, 3187 (2006).
[9] M. Burriel, C. Niedrig, W. Menesklou, S.F. Wagner, J. Santiso and E. Ivers-Tiffée, Solid State Ionics, 181, 602 (2010).
[10] J.A. Thornton, Ann. Rev. Mater. Sci., 7, 239 (1977).
[11] S. Švarcová, K. Wiik, J. Tolchard, H.J.M. Bouwmeester and T. Grande, Solid State Ionics, 178, 1787 (2008).
[12] C. Niedrig, S. Taufall, M. Burriel, W. Menesklou, S.F. Wagner, S. Baumann and E. Ivers-Tiffée, Solid State Ionics, 197, 25 (2011).
[13] D.N. Mueller, R.A. De Souza, T.E. Weirich, D. Roehrens, J. Mayerb and M. Martina, Physical Chemistry Chemical Physics, 12, 10320 (2010).
[14] M. Arnold, T.M. Gesing, J. Martynczuk and A. Feldhoff, Chem. Mater., 20, 5851 (2008).
[15] A.A. Yaremchenko, S.M. Mikhalev, E.S. Kravchenko and J.R. Frade, http://dx.doi.org/10.1016/j.jeurceramsoc.2013.09.012
[16] X. Li, T. Kerstiens and T. Markus, Journal of Membrane Science, 438, 83 (2013).
[17] P. Müller, H. Störmer, L. Dieterle, C. Niedrig, E. Ivers-Tiffée and D. Gerthsen, Solid State Ionics, 206, 57 (2012).
[18] M.M. Kuklja, Y.A. Mastrikov, B. Jansang and E.A. Kotomin, Solid State Ionics, 230, 21 (2013).
[19] S. McIntosh, J.P.Vente, W.G. Haije, D.H.A. Blank and H.J.M. Bouwmeester, Chem.Mater., 18, 2187 (2006).
[20] R.B. Hetnarski and M.R. Eslami, Thermal Stresses-Advanced Theory and Applications, Springer, Berlin, 2009.
[21] O. Madelung, U. Rössler and M. Schulz (Eds.), Magnesium oxide (MgO) crystal structure, lattice parameters, thermal expansion, Landolt-Börnstein - Group III Condensed Matter, Springer, Berlin, 1999.
[22] B.X. Huang, J. Malzbender, R.W. Steinbrech, P. Grychtol, C.M. Schneider, and L. Singheiser, App. Phys. Lett., 95, 051901 (2009).
[23] B.X. Huang, J. Malzbender, R.W. Steinbrech and L. Singheiser, J. Membr. Sci., (2009), doi:10.1016/j.memsci.2009.08.026.
[24] J. Ovenstone, J. Jung, J.S. White, D.D. Edwards and S.T. Misture, J. Solid State Chem., 181, 576 (2008).
[25] S. Li, Z. Lü, X. Huang and W. Su, Solid State Ionics, 178, 1853 (2008).